Applied Energy 185 (2017) 280–293

Contents lists available at ScienceDirect

Applied Energy

journal homepage: www.elsevier.com/locate/apenergy

Examination of the optimal operation of building scale combined heat and power systems under disparate climate and GHG emissions rates

B. Howard *, V. Modi

Department of Mechanical Engineering, Columbia University, 500 W 120th St, New York, NY 10027, United States

HIGHLIGHTS

- CHP attributable reductions, not viable by electric generation alone, are defined.
- Simplified operating strategy heuristics are optimal under specific circumstances.
- Phosphoric acid fuel cells yield the largest reductions except in the extremes.
- Changes in baseline emissions affect the optimal system capacity and operating hours.

ARTICLE INFO

Article history:
Received 18 April 2016
Received in revised form 26 September 2016
Accepted 27 September 2016
Available online 7 November 2016

Keywords:
Building scale combined heat and power
Greenhouse gas emissions
Controlled random search
Mixed integer linear programming

ABSTRACT

This work aims to elucidate notions concerning the ideal operation and greenhouse gas (GHG) emissions benefits of combined heat and power (CHP) systems by investigating how various metrics change as a function of the GHG emissions from the underlying electricity source, building use type and climate. Additionally, a new term entitled "CHP Attributable" reductions is introduced to quantify the benefits from the simultaneous use of thermal and electric energy, removing benefits achieved solely from fuel switching and generating electricity more efficiently.

The GHG emission benefits from implementing internal combustion engine, microturbines, and phosphoric acid (PA) fuel cell based CHP systems were evaluated through an optimization approach considering energy demands of prototypical hospital, office, and residential buildings in varied climates. To explore the effect of electric GHG emissions rates, the ideal operation of the CHP systems was evaluated under three scenarios: "High" GHG emissions rates, "Low" GHG emissions rates, and "Current" GHG emissions rate for a specific location.

The analysis finds that PA fuel cells achieve the highest GHG emission reductions in most cases considered, though there are exceptions. Common heuristics, such as electric load following and thermal load following, are the optimal operating strategy under specific conditions. The optimal CHP capacity and operating hours both vary as a function of building type, climate and GHG emissions rates from grid electricity. GHG emissions reductions can be as high as 49% considering a PA fuel cell for a prototypical hospital in Boulder, Colorado however, the "CHP attributable reductions are less than 10%.

1. Introduction

Combined heat and power (CHP) systems are a type of distributed generation technology where electricity and thermal energy are produced and consumed. CHP systems are based on electricity generation systems, such as internal combustion engines, gas turbines and fuel cells. In a CHP arrangement, these systems are equipped with heat recovery systems to allow the waste heat to supply a nearby thermal demand.

Distributed generation systems, including those with CHP systems, have been deemed advantageous for a variety of reasons. Major benefits potentially include the deferment of large investments in the electric transmission and distribution infrastructure, increase in grid reliability and power quality if ideally located, and more efficient use of resources with the use of CHP configurations [1–4]. As more efficient use of resources results in greenhouse gas (GHG) emissions reductions, CHP systems have been promoted by many policymakers in the United States and Europe [5–8].

However, the geographic scales of use for CHP systems have become increasingly smaller. Original uses were in industrial or

* Corresponding author.
E-mail address: bnh2111@columbia.edu (B. Howard).

http://dx.doi.org/10.1016/j.apenergy.2016.09.108
0306-2619/

Nomenclature

$\overline{\eta_{el}}$	CHP nominal electrical efficiency
η	CHP efficiency
X	CHP electrical capacity
f_t	CHP system fuel consumption in time step t
d_l	efficiency degradation at load l
d_f	efficiency degradation at load f
p_t^h, p_t^l	piecewise linear power output of the CHP system in time step t
q_t	CHP system thermal output in time step t
be	break-even GHG emissions rate for grid electricity
e_b	GHG emissions coefficient for thermal energy produced from an on-site boiler (g CO_2e/kW h)
e_{ng}	GHG emissions coefficient for natural gas (g CO_2e/kW h)
η_{el}	CHP electrical efficiency
e_g	GHG emissions coefficient of electricity from the grid (g CO_2e/kW h)
e_b	GHG emissions coefficient for thermal energy produced from an on-site boiler (g CO_2e/kW h)
E_t	electricity demand of the building in time step t
H_t	thermal demand of the building in time step t
e_t	electrical energy produced by the CHP system and used by the building in hour t
h_t	thermal energy produced by the CHP system and used by the building in hour t
w_t	binary variable defining piecewise linear CHP power output
μ_t	operating status of the CHP system in hour t
Δ	search range in kW for controlled random search algorithm
ϕ	probability of accepting a solution with poor objective function for controlled random search

district energy systems that utilized waste heat to serve large thermal demand centers. More recently CHP systems have been implemented at the building level to meet local electricity, space heating and water heating demands [9,10]. However with diminished size comes additional challenges.

At the building scale, the electric and thermal demands are more variable over the year, as one can not leverage the smoothing that occurs with the aggregation of building demands. Moreover, performance parameters diminish with size, potentially impacting the GHG emissions benefits for buildings with lower energy demands [11]. In consequence determining the proper prime mover, capacity, and operational strategy, i.e. the output of the CHP system in each time step, becomes increasing important and complex.

This has led to a large body of research analyzing the how to best operate CHP system under various sets of conditions [12–16,5,17–28]. "Best" has been defined in many ways including minimal cost, energy consumption, GHG emissions and exergy efficiency. The disparate conditions include climatic conditions, energy cost structures, CHP system characterizations, and GHG emissions from the baseline system. In this work we focus on CHP systems operated to minimize GHG emissions, thus we review a select set of papers that have evaluated the impacts on this criteria. Table 1 describes the scenarios explored in several studies on CHP systems, specifically highlighting the building use cases, climate zone, CHP system type (prime mover), GHG emissions from baseline scenarios, operating strategy, sizing strategy and resulting conclusions.

A range of building use cases, or building types, have been considered from industrial, commercial, and residential. However studies considering the largest diversity of building types typically considered the effects in a single climate under fixed GHG emissions rates from grid electricity and thermal demands [17,25]. Conversely Mago et al. [15] evaluated the performance of CHP systems in various climates but only considered a single use case. Additionally both research teams used a simplified operating and sizing strategies that do not result in the largest GHG emissions reductions. Operating strategies vary from heuristics such as continuous output, electrical load following, thermal load following, and maximum output. For the heuristics, the operating strategy is determined without consideration of the demand. Optimal strategies attempt to determine the best way to operate a system taking into account the building demands and constraints on the CHP systems themselves. Each of these strategies from heuristics to optimal linear, mixed-integer linear and nonlinear programs has been used to estimate GHG emissions savings from CHP systems. Moreover, researchers have compared the optimal approaches to the heuristics, resulting in mixed findings. Ghadimi et al. [24] found that the optimal approach was well approximated by the electric load following heuristic. Yet Hueffed and Mago [17] have found that neither the electric load following or a thermal load following approach could match the reductions in the optimal case. Lastly very few researchers in the studies reviewed search for the optimal size of the CHP system. More commonly the system capacity is determined a priori.

In the studies reviewed, the GHG emissions reductions from implementing CHP systems ranged from 0–52%. With the many and varied evaluations, it is difficult to discern how different factors such as building type, climate, prime mover, and grid GHG emissions rates affect the GHG emissions benefits of CHP systems.

Another aspect not addressed in other studies is quantifying the *added* benefit of the combined heat and power operation. For example Hueffed and Mago [29] consider arguably high values of GHG emissions from grid electricity and find reductions up to 52%. Given this high GHG emissions rate from grid electricity, it is unclear how much benefit comes from operating in combined heat and power mode versus switching to a low carbon fuel and generating electricity at a higher efficiency.

The aim of this analysis is to clarify and unify statements made in previous works about CHP systems by determining how the optimal operating strategy, operating hours, system capacity, and ideal CHP system type change as a function of the GHG emissions from the underlying electricity source considering a broad range of building types and climates. We seek to provide analysis that can be generalized to allow for an easier understanding of how CHP systems should be sized and operated to reduce GHG emissions. In addition, this work defines a new term, CHP attributable reductions, that quantifies the amount of savings that are specifically due to the simultaneous use of thermal and electrical energy produced by a CHP system.

The analysis is performed by finding, through an optimal sizing and dispatch program, the CHP system that maximizes GHG emissions reductions for prototypical hospitals, office and residential buildings, of different sizes, in 16 climates, under "high" and "low" GHG emissions scenarios. The results of the optimization are explored to draw general conclusions about the reduction potential, ideal prime mover, CHP system capacities and operational strategies under the various scenarios. "CHP attributable" GHG emissions reductions are defined by considering the difference between two optimizations: one where the objective function

Table 1
Description of selected studies on the operation of CHP systems.

Study	Use case	Climate zone[a]	CHP system	GHG emissions rate	Operating strategy	Sizing strategy	Conclusions
Ren and Gao [21]	Residential	Mixed-humid	ICE, fuel cells	E: 370 g CO_2/kW h; T: 229 g CO_2/kW h	Emission optimal mixed-integer linear program	Fixed 1 kW systems	1–9 CO_2 emission reductions
Ghadimi et al. [24]	Industrial plant	Not specified	ICE	E: 978 g CO_2e/kW h; T: 247–617 g CO_2e/kW h	Continuous, electric load following, thermal load following, GHG optimal non-linear optimization	Search space at 100 kW increments	28% GHG emissions reductions, Optimal approach and electric load following yield equal GHG savings
Mago et al. [15]	Hospital	All climate zones	Generic prime mover	E: 328–854 g CO_2/kW h; T: not specified	Continuous	Various sizes related to electricity and thermal demands of the building	0–17.2% CO_2 emission reductions
Mago and Smith [17]	Various	Cold	Generic prime mover	E: 533 g CO_2e/kW h; T: 200 g CO_2e/kW h	Continuous	Capacity equal to 30% average hourly demand	16–21% GHG emissions reductions
Howard et al. [25]	Various	Mixed-humid	ICE, microturbines	E: 561 g CO_2e/kW h; T: 239 g CO_2e/kW h	Electric load following	30–3000 kW, search space at 1 kW increments	Average GHG emissions reductions 16%
Hawkes and Leach [13]	Residential	Marine	ICE, fuel cell, stirling engine	E: 430 g CO_2/kW h; T: 189 g CO_2/kW h	Electric load following, thermal load following, cost-optimal quadratic programming	Fixed 2 kW systems	21% reduction with optimal dispatch, heat-led strategy can be better for GHG emissions than cost optimal
Hueffed and Mago [29]	Small office	Cold-very cold	ICE (CCHP)	E: 789–1230 g CO_2/kW h; T: 188 g CO_2/kW h	Constant dispatch, electrical load following, thermal load following, GHG optimal linear program	Fixed sizes of 6, 8.5 and 12 kW	9–52% CO_2 emission reductions, GHG optimal provides larger reductions than all other heuristics
Wang et al. [30]	Hotel	Hot-humid	Microturbine (CCHP)	E: 877–968 g CO_2/kW h; T: 185–255 g CO_2/kW h	Electric load following, thermal load following	Fixed size	9–25% CO_2 emission reductions

ICE: Internal Combustion Engine, CCHP: Combined Cooling Heating and Power, E: GHG (or CO_2) emissions rate from the electricity source, T: GHG (or CO_2) emissions rate from the thermal energy source.
[a] Climate zones estimated to equivalent US Department of Energy Building America climates zones [31].

includes considerations for both thermal and electric demands and one where only savings from electricity production are considered.

The remainder of this paper is organized as follows: Section 2 describes the governing systems including the building energy demands as a function of building type and climate, greenhouse gas emissions rates from electric and thermal energy production, and CHP technologies and performance parameters. Section 3 describes the break-even point for GHG emissions reductions from CHP systems. Section 4 describes the mixed integer linear program and controlled random search algorithm utilized to determine the optimal capacity and operational strategy. Section 5 describes and discusses the results of the analysis and Section 6 provides the final remarks and conclusions.

2. Defining the governing systems

For the analysis, a single building is considered with thermal and electric energy demands that can be satisfied by a local CHP system, on-site boiler, or electricity provided through the regional power grid. The following sections define the building energy demands, the GHG emissions produced from thermal and electricity energy sources, and the CHP system performance characteristics.

2.1. Building electric and thermal energy demands

The building energy demands used in this analysis were those simulated for the DOE commercial building benchmark buildings [32]. The goals of the simulations, performed in EnergyPlus, are to provide an estimate of the energy demands of different building types in various climates behave on average. More specifically the electricity, space heating, and water heating demands for the hospital, large office (office) and mid-rise residential (residential) building types for 16 cities representing various climate regions were simulated. The climate regions across the United States are defined by the building performance association into 8 different regions: Hot-Dry, Hot-Humid, Mixed-Humid, Mixed-Dry, Marine, Cold, Very Cold, and Subarctic. Full descriptions of the climate regions can be found in [31]. Using these simulations allows for exploration of the effects of both building usage and climate.

One of the aims of this analysis is to determine GHG emissions reductions as a function of building size. Building size in this analysis, is proxy for the *magnitude* of the building energy demands. Therefore to maintain a common point of reference, the total annual building energy demands were scaled to two different values: 10^7 kW h per year and 10^6 kW h per year representing "Large" and "Small" buildings respectively. In each scenarios, the annual energy demand of each building across all building types is the same however the relative magnitude of the thermal (space and water) and electricity demands are different. This allows for a direct comparison alleviating the influence of the relative energy demands as a function of size for each building. The simulated annual non-cooking energy consumption by electric, space heating, and water heating demands for each location are shown in Table 2.

It should be noted that by adjusting the annual energy demands, the physical size of the buildings are changing as well if one considers the building's energy intensity to be constant. The large buildings could be between 450,000 and 1,200,000 sq. ft. for residential buildings, 500,000–850,00 sq. ft. for office buildings, and 185,000–250,000 sq. ft.

2.2. GHG emissions from electricity and thermal production

In the United States, electricity is typically provided through the electric grid from a slew of power plants each having their own

Table 2
Percent annual electricity, space heating, and water heating demand by city and climate zone for hospital, office and residential buildings.

Climate zone	City	% Annual non cooling energy demand								
		Office			Multi-family residential			Hospital		
		E	SPH	WH	E	SPH	WH	E	SPH	WH
Subarctic	Fairbanks, AL	46.2	53.1	0.7	17.6	74.9	7.5	58.2	40.1	1.7
Very cold	Duluth, MN	61.3	37.9	0.8	23.1	67.6	9.3	68.7	29.7	1.6
Cold	Minneapolis, MN	68.4	30.9	0.7	27.8	62.6	9.6	71.3	27.3	1.4
Cold	Mt. Helena, MT	72.9	26.3	0.8	29.5	59.6	10.9	73.7	24.7	1.6
Cold	Chicago, IL	75.5	23.8	0.7	31.8	58.0	10.2	73.7	25.0	1.3
Cold	Boulder, CO	82.0	17.2	0.8	36.1	52.0	12.0	77.7	20.8	1.5
Marine	Seattle, WA	74.7	24.5	0.7	34.1	54.2	11.7	71.6	27.1	1.3
Marine	San Francisco, CA	87.4	11.8	0.8	44.9	40.3	14.8	74.0	24.7	1.3
Mixed-dry	Albuquerque, NM	84.8	14.5	0.7	45.0	42.8	12.2	78.0	20.7	1.3
Mixed-humid	Baltimore, MD	79.4	20.0	0.6	37.9	51.7	10.5	74.3	24.6	1.1
Mixed-humid	Atlanta, GA	87.2	12.2	0.5	49.8	38.7	11.5	76.5	22.5	1.0
Hot-dry	Phoenix, AZ	84.5	5.1	0.4	74.4	15.9	9.7	78.5	20.7	0.8
Hot-dry	Las Vegas, NV	91.7	7.8	0.5	62.7	26.6	10.7	77.9	21.1	1.0
Hot-dry	Los Angeles, CA	94.4	5.0	0.6	64.1	18.7	17.1	77.2	21.7	1.1
Hot-humid	Houston, TX	93.1	6.5	0.5	66.6	22.4	11.0	78.8	20.3	0.9
Hot-humid	Miami, FL	98.5	1.1	0.4	88.3	1.7	10.1	81.3	17.9	0.8

E: Electricity demand, SPH: Space Heating demand, WH: Water Heating demand.

GHG emissions characteristics. The simplest approximation, and the one utilized in this work, is to define the GHG emissions produced by a set of power plants by an average GHG emission rate, or the grams of GHG emissions (in carbon dioxide equivalent) produced per kW h of electricity produced annually.

Average GHG emission rates have been estimated for different regions across the United States by the EPA in their emissions and generation integrated database (eGRID). They make estimates for varying geographic scales from the state to the whole of the US. The eGRID estimates do not account for transmission across the geographic boundaries, only the emissions from power plants physically located in that region. This can lead to skewed estimates if a particular state relies on the generation of a neighboring region. To mitigate that effect, the GHG emissions rates for the buildings in each of the 16 cities were defined by their corresponding eGRID primary subregions. The cities and their corresponding electric GHG emissions rate is shown in Table 3.

However in this work we also seek to determine how the GHG emissions from electricity production effect how one would size and operate a CHP system. Therefore we also define two generic GHG emissions scenarios for which we will evaluate the results of each system. The first scenario is termed the "High" GHG emissions scenario. In this scenario the GHG emissions rate from grid electricity is set to 750 g CO_2e/kW h. To provide a specific example, this rate represents an electricity system where 60% is provided by a typical coal power plant and 40% is provided by a natural gas power plant, considering average US power plant efficiency by fuel source. The second scenario is termed the "Low" GHG emissions scenario, where the GHG emissions rate from grid electricity is defined as 300 g CO_2e/kW h. This scenario represents an electricity system where 70% is provided by natural gas power plants and 30% from renewable sources. Considering the values in Table 3, these two scenarios do indeed represent "High" and "Low" GHG emission rates.

For thermal energy production, many commercial and residential buildings in the United States use natural gas boilers or furnaces [33]. Boilers are very efficient at converting natural gas into thermal energy with factory efficiencies up to 90%. With wear and tear however the efficiencies diminish over time. In this work, the boiler thermal efficiency was assumed to be 80% leading to a GHG emission rate of 225 g CO_2e/kW h. This assumption holds true for all scenarios considered in this work.

Table 3
16 simulated building locations and the corresponding NERC subregion GHG emissions rates.

City	NERC subregion GHG emissions rate (g CO_2e/kW h)
Fairbanks, AL	582
Duluth, MN	725
Minneapolis, MN	725
Mt. Helena, MT	725
Chicago, IL	693
Boulder, CO	831
Seattle, WA	169
San Francisco, CA	300
Albuquerque, NM	542
Baltimore, MD	432
Atlanta, GA	432
Phoneix, AZ	542
Las Vegas, NV	542
Los Angeles, CA	300
Houston, TX	537
Miami, FL	535

2.3. CHP technology characterization

This section provides a brief overview of CHP systems, the parameters use to characterize them, and how the performance was mathematically defined for the subsequent optimization.

The CHP systems evaluated are those applicable at the building scale. The main considerations were system size and load following capability. In a load following operating scheme, the CHP system is expected to modulate its output to meet demands. These constraints led to the consideration of three different types of CHP systems: microturbines, internal combustion engines, and phosphoric acid (PA) fuel cells all fueled by natural gas.

The main characteristics to describe the operation of a CHP system are the nominal electrical efficiency (η_{el}), CHP efficiency (η), electrical capacity (X), and part load efficiency. The nominal electrical efficiency is the ratio of electricity produced to the energy content of the fuel source at maximum capacity. The CHP efficiency is the ratio of the aggregate useful thermal and electrical energy to the energy content of the fuel source. The electrical capacity is the maximum electrical power output of the CHP system. Lastly the part-load efficiency, defined by more than one parameter, describes the degradation of the efficiency when not operating at the full electrical capacity.

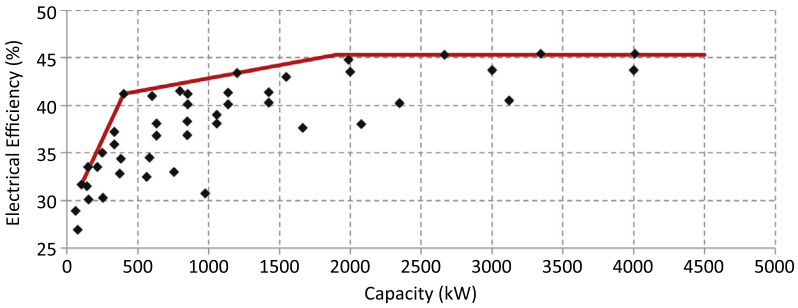

Fig. 1. Electrical efficiency as a function of electrical capacity from various manufacturing specifications for thermal systems. Maximum efficiency as defined by a piecewise linear function is shown in red.

The thermal systems and the electrochemical systems differ in the relationship between these parameters.

2.3.1. Nominal electrical efficiency and system capacity

For internal combustion systems, the nominal electrical efficiency is a function of the electrical capacity (or the system size). More specifically the electrical efficiency decreases as the capacity decreases due to increased mechanical losses. To capture this dependence, the nominal electrical efficiencies for internal combustion engines of various sizes were collected from manufacturing specifications [34,34–36]. As illustrated in Fig. 1, the nominal electrical efficiency increases rapidly until approximately 400 kW, slowly increases between 400 kW and 2000 kW, and then plateaus to around a constant 45% electrical efficiency.

This dependency was modeled as a piecewise linear curve considering only the highest efficiencies at a given capacity which is also visualized in Fig. 1. The mathematical relationship is described as follows

$$\overline{\eta_{el}}(X) = \begin{cases} 3.2 * 10^{-4} X + .287, & X \leqslant 401 \\ 2.6 * 10^{-5} X + .402, & 401 < X \leqslant 1990 \\ 0.453, & X > 1990 \end{cases} \quad (1)$$

where X, the electric capacity, is in kW and $\overline{\eta_{el}}$ is the nominal electrical efficiency. Characterizing the relationship between the nominal electrical efficiency and system capacity as a continuous function is done to allow for ease of computation.

The same procedure was followed for microturbine systems [37,38] resulting in the following piecewise linear curve

$$\overline{\eta_{el}}(X) = \begin{cases} 7.4 * 10^{-4} X + .238, & 30 < X \leqslant 125 \\ 0.33, & X > 125 \end{cases} \quad (2)$$

Fuel cell systems operate under different principles than thermal systems. The capacity of a fuel cell systems is created by stacking individual cells of low voltage in series. This decouples the electrical efficiency from the size. This can be seen in commercial products with PureCell [39] offering a 5 kW and 400 kW PA fuel cells with nominal electrical efficiencies of 40% and 42%, respectively. This differs for thermal system where the electrical efficiency could change from 30% to over 40% over the same range (see Fig. 1). Therefore fuel cell systems were modeled with constant nominal electrical efficiency of 40% over all sizes.

2.3.2. Part-load electrical efficiency

In addition to the electrical efficiency changing as a function of size, for all systems considered the electrical efficiency reduces when not operating at the maximum capacity. Fig. 2 depicts typical efficiency reduction as a function of part load for fuel cells, internal combustion engines and microturbines reproduced from [11].

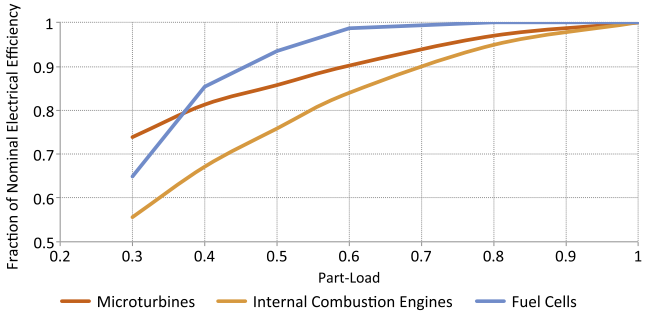

Fig. 2. Typical part-load electrical efficiency degradation for fuel cells, internal combustion engines, and microturbines [11].

Each of the systems has slightly different part-load behavior. Fuel cells can maintain their nominal electrical efficiency until approximately 60% of the rated capacity after which the efficiency degrades rapidly. For microturbines and internal combustion engines the efficiencies slowly degrade with internal combustion engines having more severe degradation.

The fuel consumption as a function of load is called the heat rate. The part-load efficiencies were converted to heat rates and those heat rates were modeled as piece-wise linear curves defined by two segments that describe the operation in "low" and "high" output regimes. Given this definition the fuel consumption of the system is defined as follows

$$f_t = A^h p_t^h + A^l p_t^l + B\mu_t \quad (3)$$

where

$$A^h = \frac{1 - \frac{1}{d_f}}{\overline{\eta_{el}}(1 - f)} \quad (4)$$

$$A^l = \frac{\frac{1}{d_f} - \frac{1}{d_l}}{\overline{\eta_{el}}(f - l)} \quad (5)$$

$$B = \frac{X}{\overline{\eta_{el}}}\left[\frac{1}{d_l} - \frac{l}{f - l}\left(\frac{1}{d_f} - \frac{1}{d_l}\right)\right] \quad (6)$$

In the equations above d_l and d_f are the efficiency degradation at part-loads l, and f, respectively. Due to the piecewise linear formulation, the power output of the CHP system has been defined by two variables p_t^h and p_t^l that when summed equal the total output electrical energy output of the CHP system in timestep t.

By letting the CHP efficiency η be constant over all loads, we can also define the thermal output of the CHP system as follows

$$q_t = \eta\left(A^h p_t^h + A^l p_t^l + B\mu_t\right) - p_t^h - p_t^l \quad (7)$$

Table 4
CHP system performance parameters, [39,37,38,36].

Parameter	Microturbines	Internal combustion engines	PAFC
l	0.3	0.3	0.3
f	0.8	0.8	0.6
d_l	0.75	0.55	0.75
d_f	0.97	0.95	1.0
η	0.90	0.85	0.9

Table 5
Break-even electric GHG emissions rates for thermal and fuel cell CHP systems.

System type	Break-even emissions (g CO_2e/kW h)
Microturbines	115–160
Internal combustion engines	161–202
PA fuel cells	153–171

For each system type considered the part-load performance parameters are shown in Table 4.

3. Break-even GHG emissions rates

An avoided burden approach was used to estimate the GHG emissions reductions from implementing CHP systems. This approach estimates the GHG emissions that would have been produced from the current method of electricity and thermal energy generation and subtracts the estimated GHG emissions produced from the CHP operation. The difference is considered the GHG emissions savings.

With the fuel source and efficiency of the CHP system and the GHG emissions rate for thermal energy production defined, one can determine the GHG emission rate from electricity production for which a CHP system will have zero impact on GHG emissions. This value, or the break-even point, is calculated as follows

$$be = \frac{e_{ng}}{\eta_{el}} - \frac{e_b * (\eta - \eta_{el})}{\eta_{el}} \tag{8}$$

where be is the break-even GHG emissions rate for grid electricity, e_b is the GHG emissions coefficient for thermal energy produced from an on-site boiler (g CO_2e/kW h), e_{ng} is the GHG emissions coefficient for natural gas (g CO_2e/kW h), η is the total CHP efficiency, and η_{el} is the CHP electrical efficiency. As the electrical efficiencies vary as a function of capacity and load, the break-even GHG emission rates are defined for the range of efficiencies possible for each system type and are shown in Table 5. These values define the value of GHG emissions from grid electricity for which a CHP system would neither increase of decrease GHG emissions.

4. Estimation methodology

Given the governing systems defined in Section 2, the task is to now for each set of building energy demands determine the system capacity and operating strategy that minimizes the overall GHG emissions. Allowing the nominal electrical efficiency to be a function of the capacity while also defining the part-load efficiency, however, leads to a complex problem formulation. In fact Eqs. (1) and (3), lead to a mixed-integer nonlinear optimization program. However if one defines the system capacity a priori, the problem can be formulated as an easy to solve mixed-integer linear program(MILP). This decoupling allows one to search the solution space for the capacity that minimizes GHG emissions. This is the basis of a simple global optimization technique called controlled random search (CRS). Sections 4.1 and 4.2 describe the MILP formulation and the CRS algorithm, respectively. Section 4.3 describes how the CHP attributable GHG emission reductions were calculated.

4.1. Operating strategy: mixed-integer linear program

The operating strategy is decided by a mixed-integer linear program where the objective function is to maximize GHG emissions reductions considering GHG emissions from grid electricity, on-site boiler and combined heat and power system. The full program is described in the following equations

Objective Function

$$max \sum_{t \in T} (e_g e_t + e_b h_t - e_{ng} f_t) \tag{9}$$

Subject to

$$0 \leqslant e_t \leqslant E_t \ \forall t \in T \tag{10}$$

$$0 \leqslant h_t \leqslant H_t \ \forall t \in T \tag{11}$$

$$0 \leqslant e_t \leqslant p_t^h + p_t^l \ \forall t \in T \tag{12}$$

$$0 \leqslant h_t \leqslant q_t \ \forall t \in T \tag{13}$$

$$\mu_t Xl \leqslant p_t^h + p_t^l \leqslant \mu_t X \ \forall t \in T \tag{14}$$

$$\omega_t fX \leqslant p_t^l \leqslant fX \ \forall t \in T \tag{15}$$

$$0 \leqslant p_t^h \leqslant X(1-f)\omega_t \ \forall t \in T \tag{16}$$

$$\mu_t, \omega_t \in [0,1] \tag{17}$$

$$p_t^h, p_t^l, h_t, e_t \geqslant 0 \tag{18}$$

where e_g is the GHG emissions coefficient of electricity from the grid (g CO_2e/kW h), e_b is the GHG emissions coefficient for thermal energy produced from an on-site boiler (g CO_2e/kW h), E_t is the electricity demand of the building in hour t, and H_t is the thermal demand of the building in hour t.

The decision variables are the electrical energy produced by the CHP system and used by the building in hour t (e_t), the thermal energy produced by the CHP system and used by the building in hour t (h_t), and the electrical power output of the CHP system in hour t (p_t^h, p_t^l, w_t), and the operating status of the CHP system in hour t, (μ_t).

The constraints defined by Eqs. (10) and (11) ensure that the energy used by the building is not more than the electric an thermal energy demands in any hour. Eqs. (12) and (13) ensure that the energy produced by the CHP system and used by the building is less than the output of the CHP system. Eq. (14) requires the power produced by the CHP system to be within the minimum and maximum outputs. Eqs. (15) and (16) define the piecewise linear formulation of the CHP power output. Lastly Eqs. (17) and (18) define the integrality and non-negative constraints on the decision variables. This formulation allows for waste of the electric or thermal energy produced by the CHP system or to not use the system entirely if deemed advantageous.

The CHP capacity and the corresponding electrical efficiency are not decision variables in the MILP formulation. For any set of building demands the MILP described above is repeatedly solved for various values of CHP capacity. The system with the largest reductions in building GHG emissions, as found by a controlled random search as described in Section 4.2, was selected as the system capacity.

4.2. Sizing strategy: controlled random search

In this section the MILP previously described is considered a function, $MILP(X)$, that takes a system capacity as an input and outputs the GHG emissions reductions. The CRS algorithm finds the capacity that maximizes the GHG emissions reductions by systematically searching the solution space. Initially a capacity is randomly selected from a uniform distribution over an interval of $\pm\Delta$. The GHG emissions reductions the specified capacity are evaluated and recorded. If the reductions are more than the previous solution then a new capacity is selected from a uniform distribution about the new capacity. If the reductions are less than the previous solution, then the solution is discarded or accepted as a new solution with a probability ϕ. Accepting a sub-optimal solution allows the algorithm to get out of local minima. This procedure was repeated until the algorithm has not found a better solution for 20 iterations. The full controlled random search is defined by Algorithm 1.

Algorithm 1. Controlled Random Search.

```
begin
    pX ← 500
    bX ← pX
    pghg ← MILP(pX)
    bghg ← pghg
    st ← 1
    SolutionCount ← 0
    while SolutionCount < 20 do
        for i = 1 : st * Tl do
            nx ← Unif(pX − Δ, pX + Δ)
            nghg ← MILP(nX)
            diff ← nghg − pghg
            if diff > 0 then
                pX ← nX
                pghg ← nghg
                if nghg > bghg then
                    bx ← nx
                    bghg ← nghg
                    SolutionCount ← 0
            else
                q ← Unif(0, 1)
                ϕ ← exp(diff/T)
                if q < ϕ then
                    pX ← nX
                    pghg ← nghg
            SolutionCount ← SolutionCount + 1
        T ← a * T
```

4.3. Defining CHP attributable GHG emissions reductions

One of the intentions of this work is to clarify the additional benefits of CHP systems by disaggregating the GHG emissions reductions that can be achieved by electricity only systems. To that aim, once the CRS has found the capacity that minimizes GHG emissions, a second MILP program is run to calculate the GHG emissions reductions without using any of the waste heat. For that MILP the objective function is changed to

$$max \sum_{t \in T} (e_g e_t - e_{ng} f_t) \tag{19}$$

and Eqs. (11) and (13) are removed.

The "CHP Attributable" GHG emissions reductions are defined as the difference between the value of the objective function as defined by Eqs. (9) and (19).

5. Results and discussion

The maximum GHG emissions reductions for the simulated buildings and CHP system types was estimated for different values of GHG emission rates from grid electricity. The following sections describe the effect on the hourly operation of the CHP system, building size for thermal systems, CHP system type, and climate for differing values of GHG emissions rates from grid electricity. The CHP attributable reductions are calculated and discussed as well. The section finishes by evaluating the GHG emissions reductions for each simulated city considering the average GHG emissions reductions from local electricity production.

5.1. Optimal CHP systems under "High" and "Low" GHG emissions scenarios

There are several changes in the optimal sizing, operation, and GHG emission reductions under the "High" and "Low" grid electricity GHG emissions rates. To introduce the changes, the findings for a large residential building in Baltimore, MD will first reviewed.

Fig. 3(A) and (B) depict the thermal energy demand, electric energy demand, consumed CHP thermal output and consumed CHP electric output over 24 h for January 15, April 15th, and August 15th under "High" and "Low" GHG emissions rates, respectively. When the GHG emissions rate from grid electricity is "High", the CHP system is operational for every hour of the year. The output of the CHP system tracks the electricity demand and the waste heat is used whenever there is a concurrent thermal demand. This leads to GHG emissions reductions for all hours of the year. In contrast when the GHG emissions rate from grid electricity is "Low", the CHP system must simultaneously offset electric and thermal demands in sufficient magnitude to obtain GHG emissions reductions. On January 15th, where the thermal demand is significantly higher than the electricity demand, the CHP system tracks the electricity demand as all the thermal energy can be used. However for a few hours on April 15th, the electric and thermal demand is relatively low compared to the CHP system capacity. Operating the system at part-load to meet those demands would led to higher GHG emissions than the original sources of energy, therefore the system is not used. On August 15 for the entire day, there is not enough thermal demand to justify the CHP operation.

The optimal CHP system size changes as a function of GHG emissions rates as well. One CHP system is meant to provide energy over 8760 h of concurrent thermal and electric demands. If the system is over sized there will be significant waste for most of the hours from operating at part-load. If the system is undersized, there are missed reductions during times of higher demand. The optimal system balances these options to achieve the largest reductions. Therefore by changing the GHG emissions from grid electricity, both the size and the operating strategy shifts. For this example there is approximately a 100 kW difference in system capacity between the "High" and "Low" GHG emission scenarios.

Fig. 4 depicts the GHG emissions reductions for a "Large" residential building in Baltimore, MD from CHP operation (where waste heat is used) and electric only operation over a range of GHG emission rates from grid electricity. Under the "High" and "Low" GHG emission rates, the GHG emissions reduction reduces from 38% to 6%. However, under the "High" GHG emissions scenario the majority of the reductions could be achieved by simply generating electricity locally. For the example, this is generally true when GHG emissions from grid electricity are above 600 g CO_2e/

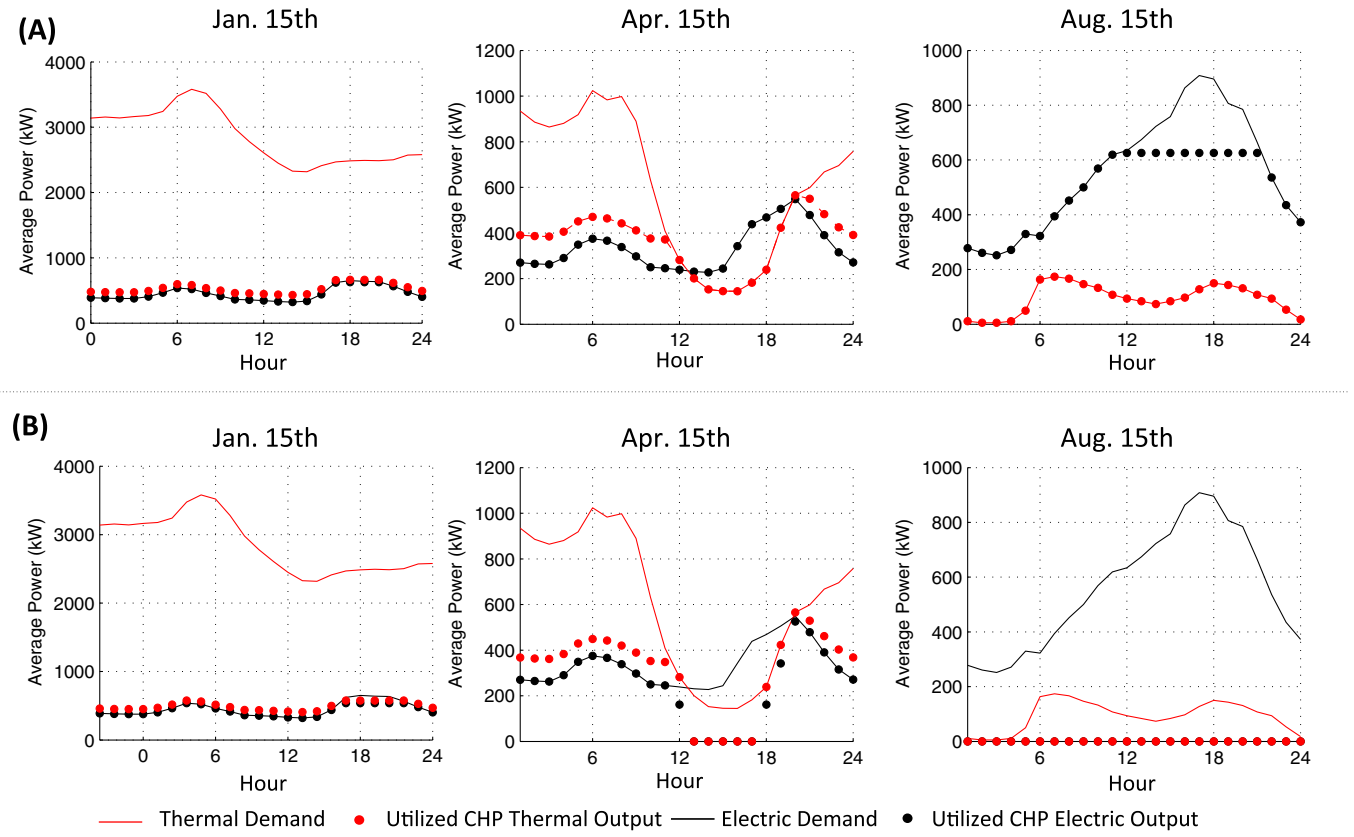

Fig. 3. Hourly dispatch of internal combustion engine driven CHP system for a large residential in Baltimore, MD (cold climate) for days in January, April and August. (A) Operation with electric grid GHG emissions rate of 750 g CO_2e/kW h, optimal system capacity: 623 kW, GHG emissions reductions: 38%. (B) Operation with electric grid GHG emissions rate of 300 g CO_2e/kW h, optimal system capacity: 527 kW, GHG emissions reductions: 6%.

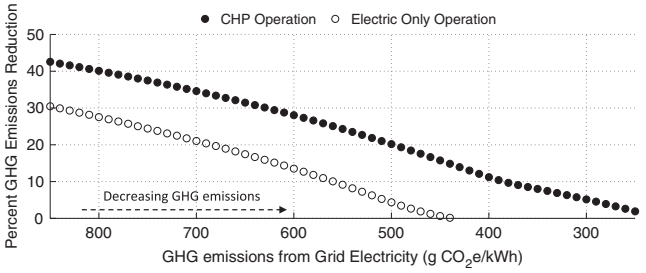

Fig. 4. GHG emissions reductions for the "Large" residential prototypical building in Baltimore, MD from CHP and electric only operation.

kW h as shown in the figure. As GHG emissions decrease, it becomes more prudent to use the waste heat to achieve GHG emissions reductions, leading the electric only systems to achieve minimal benefit. Overall though the "CHP attributable" reductions, or the difference between the electric only reductions and CHP operation reductions, stay consistent until the GHG emission rate moves toward the break-even point.

5.1.1. Prime mover selection

Fig. 5 depicts the CHP prime mover for each building type, location, and size that led to the largest GHG emissions reductions. Under most scenarios, the PA fuel cells resulted in the largest GHG emissions reductions. These systems have the highest total CHP efficiency and can achieve electrical efficiencies of 40%. As the electrical efficiency for these systems is not a function of size, PA fuel cells are best for both the large and small building sizes although there are a few exceptions.

For "Large" office buildings under the "High" GHG emissions scenario in all but the coldest climates, internal combustion engines provided the largest reductions. This is due to the higher electrical efficiencies that can be achieved by these systems and that energy demands for offices in these climates are dominated by electricity consumption. Similarly large hospital buildings, in warmer climates where electric energy demands are also above 75% of total demand, achieve the largest reductions with internal combustion engines. Under the "Low" GHG emissions scenarios where leveraging the waste heat is more crucial, microturbines achieve the highest reductions for some residential buildings in cold, very cold and subarctic climates.

5.1.2. GHG emissions reductions

The GHG emissions reductions for the "Large" building scenarios are shown in Fig. 6. As the efficiency of fuel cell systems has not been modeled as a function of size the GHG emissions reduction for the "Large" and "Small" building scenarios are similar and not depicted.

Under the "High" GHG emissions scenario, hospital and office buildings have fairly consistent savings over all climate zones with hospitals achieving the largest GHG emission reductions. The GHG emissions reductions from residential buildings vary over a much larger range as their electricity and thermal demands are much more variable and climate driven.

Under the "Low" GHG emissions scenario, all building types achieve reductions between 0 and 10%. Also the GHG emission reductions are much less than the relative change in the grid GHG emissions. As mentioned in previously, under the "Low" GHG emission scenario the operating strategy changes, requiring the system to provide simultaneous thermal and electrical demand

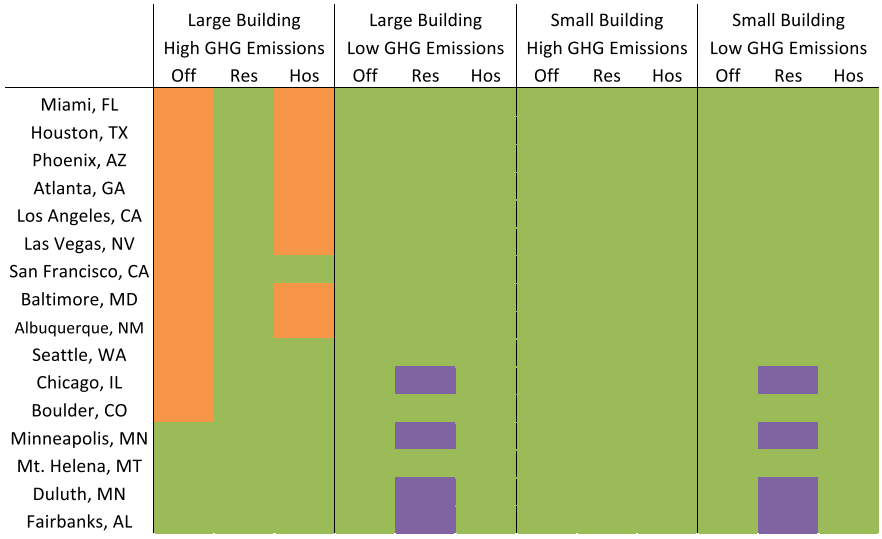

Fig. 5. CHP prime mover with largest GHG emissions reductions for each building type, location, and size under "High" and "Low" grid electricity GHG emission rates. Green: PAFC, orange: internal combustion engine, purple: microturbine. (For interpretation of the references to colour in this figure legend, the reader is referred to the web version of this article.)

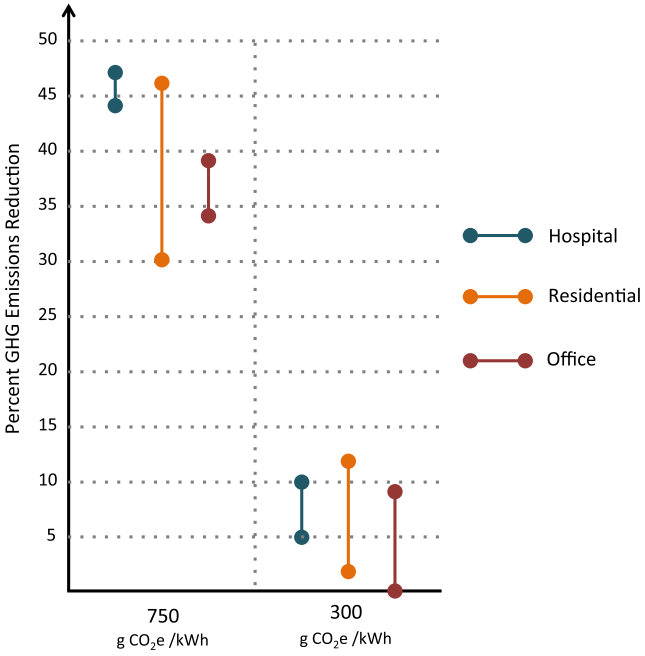

Fig. 6. GHG Emissions reductions under "High" and "Low" GHG emission rates from grid electricity. The length of the bars reflects reductions over all cities and climate zone considered.

to see reductions. This in turn reduces the operating hours and CHP system sizes leading to less overall GHG emissions reductions.

5.1.3. Operating hours and operating strategy

As the model formulation allows for a CHP system not to be operated in any given time step, it is interesting to observe the annual operating hours of the CHP system. Fig. 7 depicts the proportion of the year the optimally sized and operated CHP system supplies energy for the "Large" building types under "High" and "Low" GHG emissions rates.

Under the "High" GHG emission rate scenario, hospital and residential building types are operated throughout the year for all cli-

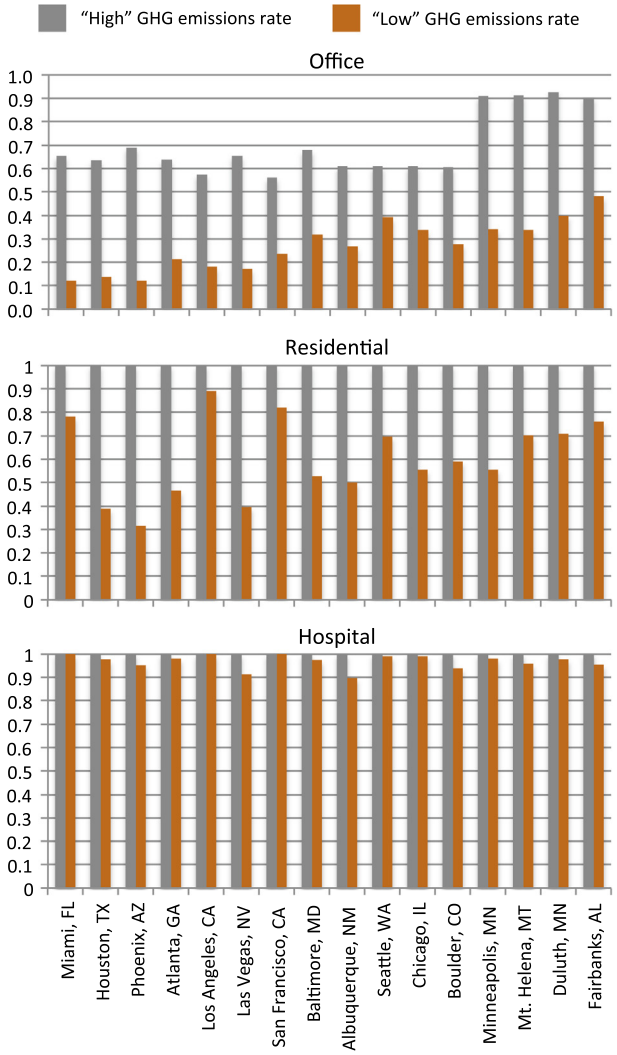

Fig. 7. Annual operation hours (proportion of the year) for "Large" office, residential, and hospital buildings under "High" and "Low" GHG emissions rates from grid electricity.

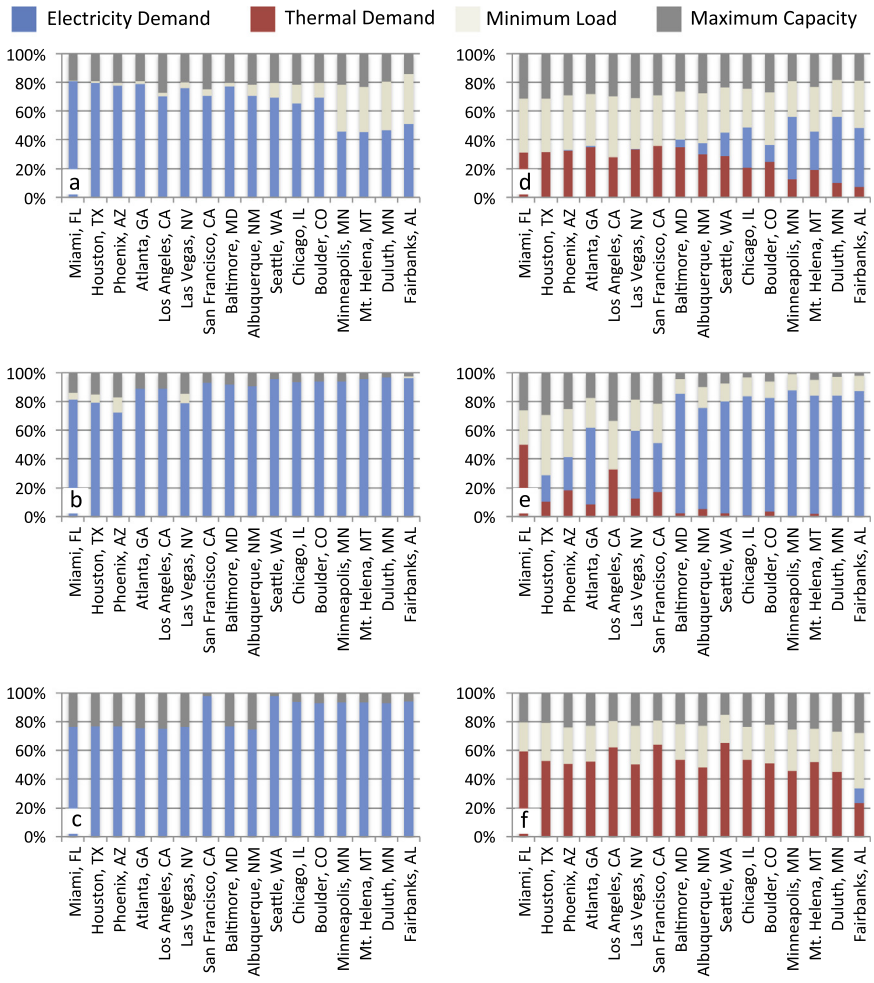

Fig. 8. Proportion of operating hours where CHP system is dispatched to meet the thermal demand, electrical demand, minimum CHP load, maximum CHP capacity. (a) Building type: office; grid electricity emissions: "High". (b) Building type: residential; grid electricity emissions: "High". (c) Building type: hospital; grid electricity emissions: "High". (d) Building type: office; grid electricity emissions: "Low". (e) Building type: residential; grid electricity emissions: "Low". (f) Building type: hospital; grid electricity emissions: "Low".

mate zones. Office buildings, however, vary in the annual operating hours due to the large variation in electrical demand. It is difficult to meet both the peaks and troughs in demand efficiently with a single system. This indicates that office buildings may be good candidates for multiple prime mover systems.

When the GHG emissions from grid electricity are low there must be a concurrent thermal demand in sufficient magnitude to achieve GHG emissions reductions or else the system is not operated. For this reason under the "Low" GHG emission rate scenarios, the annual operating hours are reduced for the office and residential building types. Hospital buildings, however, have consistent thermal and electrical demands throughout the year in all climates leading to consistently high operating hours.

Additional insights can be made by viewing how the CHP system is dispatched to meet demand. Throughout the literature various heuristics have been used define the CHP operating strategy. The most popular are electric load following and thermal load following [40,25,27,29]. The electric load following heuristic requires the CHP system to meet the electrical demand in all time steps and use waste heat if there is a concurrent thermal demand. The thermal load following heuristic designates the CHP system to meet the thermal demand in all time steps and supply electricity only if there is a concurrent demand. The optimal operating strategy could be one of those heuristics or a mixture of both.

Fig. 8 depicts the proportion of the annual operating hours that the CHP systems are dispatched to meet the electrical demand, to meet the thermal demand, at minimum part-load, or at maximum capacity. Viewing these values allows one to discern how closely the heuristics approximate the ideal operation.

Under the "High" GHG emissions rate scenario as depicted by Fig. 8(a)–(c), the CHP systems are dispatched to mainly meet the electricity demand. With the large GHG emissions coefficient, the largest reductions are achieved by meeting the electrical demand whenever possible.

Under the "Low" GHG emissions rate scenario as depicted by Fig. 8(d)–(f), the results are mixed. For Hospital buildings, the CHP systems are dispatched to mostly meet the thermal demand. CHP systems for the residential buildings in cold climates are dispatched to meet the electrical demand whereas in the warmer climates are dispatched to meet thermal demands. Lastly for Office buildings in warm climates, the CHP systems are dispatched to meet the thermal demand whereas in cold climates are dispatched to meet electrical demands. These trends occur because of the need to have a concurrent thermal and electrical demand to achieve GHG emissions reductions. Therefore the CHP systems are dispatched to meet the *lower* of the thermal and electrical demands if within the operating parameters of the CHP system.

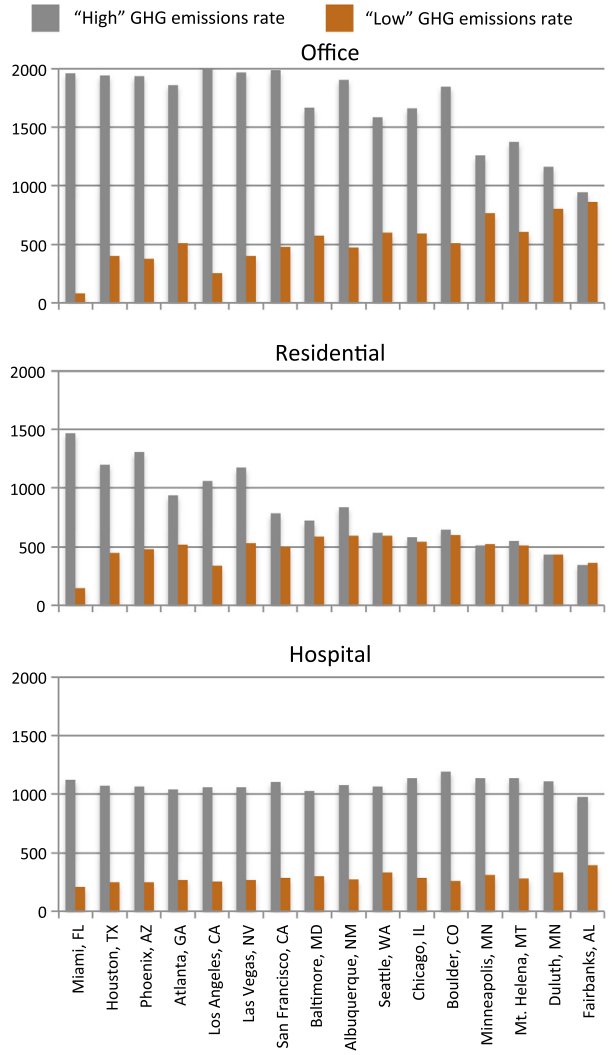

Fig. 9. Optimal CHP system capacity for the "Large" building types under "High" and "Low" GHG emissions rates from grid electricity.

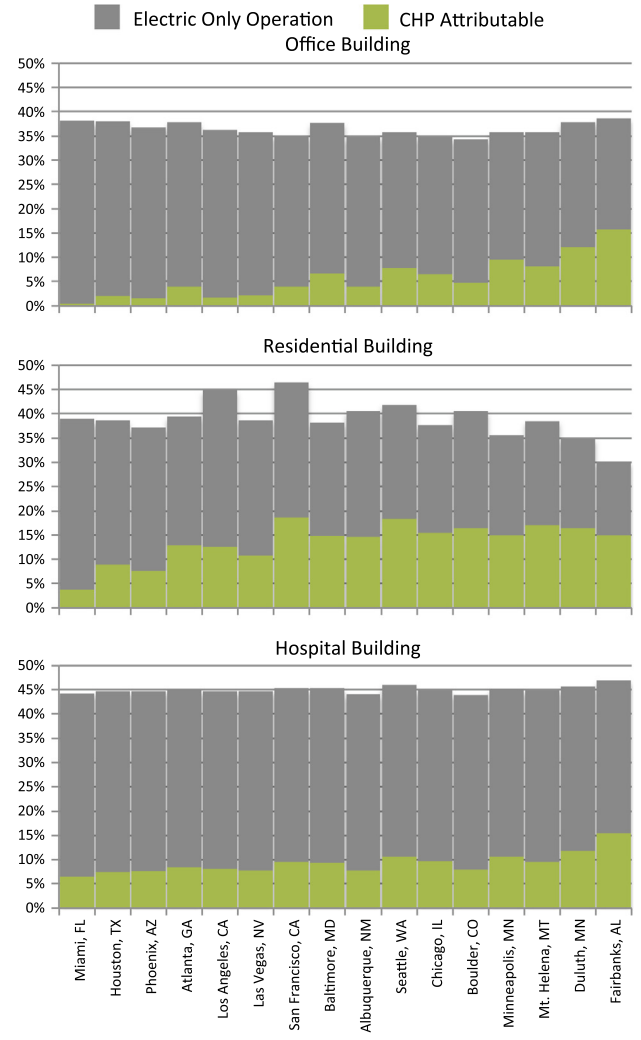

Fig. 10. CHP attributable and electric only operation GHG emissions reductions for "Large" office, residential, hospital prototypical buildings under the "High" GHG emissions scenario.

5.1.4. Optimal CHP capacity

As with the operating hours and operating strategy, the optimal system capacity changes with the GHG emissions scenario as well. Fig. 9 depicts the system capacities for the "Large" building types. Under the "High" GHG emissions scenario the systems are sized to be able to meet the larger electrical demands as this leads to the largest reductions. Under the "Low" GHG emissions scenario for the majority of building types and climates, the systems are sized smaller to obtain higher efficiencies during the times of concurrent thermal and electrical demand. The exception are the residential buildings in cold climates where the sizes do not change much between the two scenarios.

5.1.5. CHP "Attributable" GHG emissions reductions

The electric only and CHP attributable GHG emissions reductions for the large building types under the "High" GHG emissions scenario is shown in Fig. 10. While the reductions considering the contributions that can be achieved with an electric only system range between 35 and 50% for Office and Hospitals buildings, the CHP attributable reductions are less than 10% in all but the very cold and subarctic climates. Residential buildings, however, with larger thermal demands have higher CHP attributable reductions, up to 20%. These values illustrate that the reduction from electric only operation can be quite large.

Under the "Low" scenario no reductions can be achieved by an electric only system meaning all of the reductions are CHP attributable. Also as the PA fuel cell is the system of choice, the results are similar for the "Small" building size.

5.2. Optimal CHP Systems at current GHG emission rates

While the previous analyses focused on the changes in operation for specific GHG emissions scenarios, in reality each city receives electricity from a grid with it's own average GHG emission rate. To understand the implications for CHP systems under the current conditions, the optimal CHP systems were found for the location specific GHG emission rates for the "Large" building types.

The prime movers for each location that yields the largest GHG emissions reduction is shown in Fig. 11. Internal combustion engines are selected for the office and hospital building types in warm climates with higher GHG emissions rates to leverage the higher electrical efficiencies. Microturbines are selected for all building types in Seatle, WA due to the very low GHG emissions rate in that region. PA fuel cells were found to achieve the largest reductions for the remaining building types.

The GHG emissions reductions allocated into electric only and CHP Attributable contributions for each building type and location are shown in Fig. 12. With the eGRID rates, most building

Location	eGRID rate (g CO_2e/kWh)	Office	Residential	Hospital
Miami, FL	535			
Houston, TX	527			
Phoenix, AZ	542			
Atlanta, GA	604			
Los Angeles, CA	300			
Las Vegas, NV	542			
San Francisco, CA	300			
Baltimore, MD	432			
Albuquerque, NM	542			
Seattle, WA	169			
Chicago, IL	693			
Boulder, CO	831			
Minneapolis, MN	725			
Mt. Helena, MT	725			
Duluth, MN	725			
Fairbanks, AL	582			

Fig. 11. CHP prime mover with largest GHG emissions reductions for "Large" buildings under '2012 GHG emissions rates from grid electricity. Green: PAFC, orange: internal combustion engine, purple: microturbine. (For interpretation of the references to colour in this figure legend, the reader is referred to the web version of this article.)

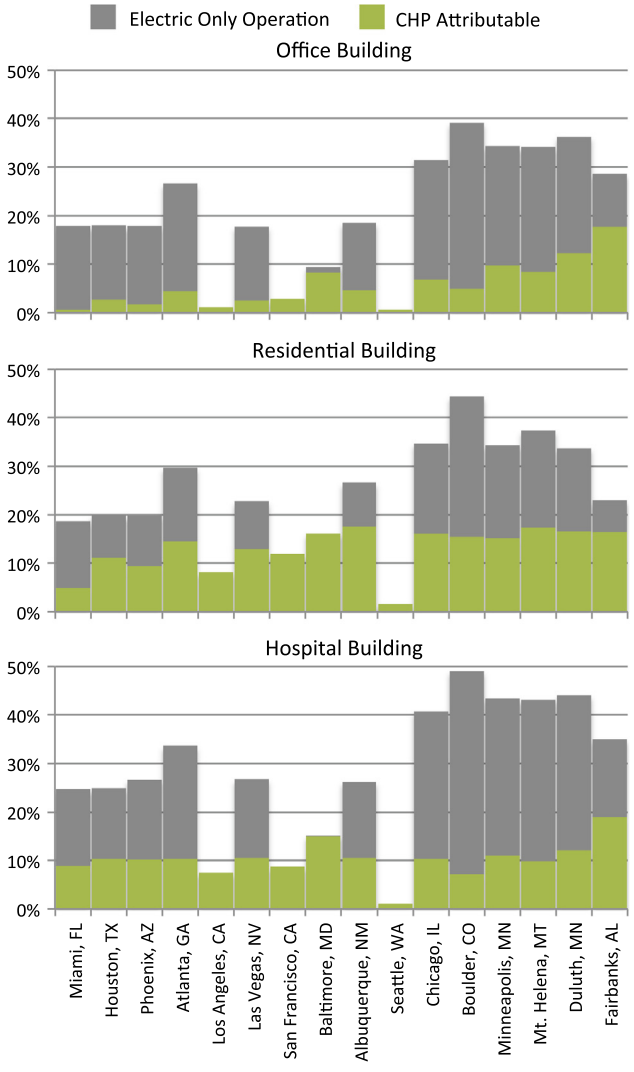

Fig. 12. CHP attributable and electric only operation GHG emissions reductions for "Large" buildings under eGRID GHG emissions rates from grid electricity.

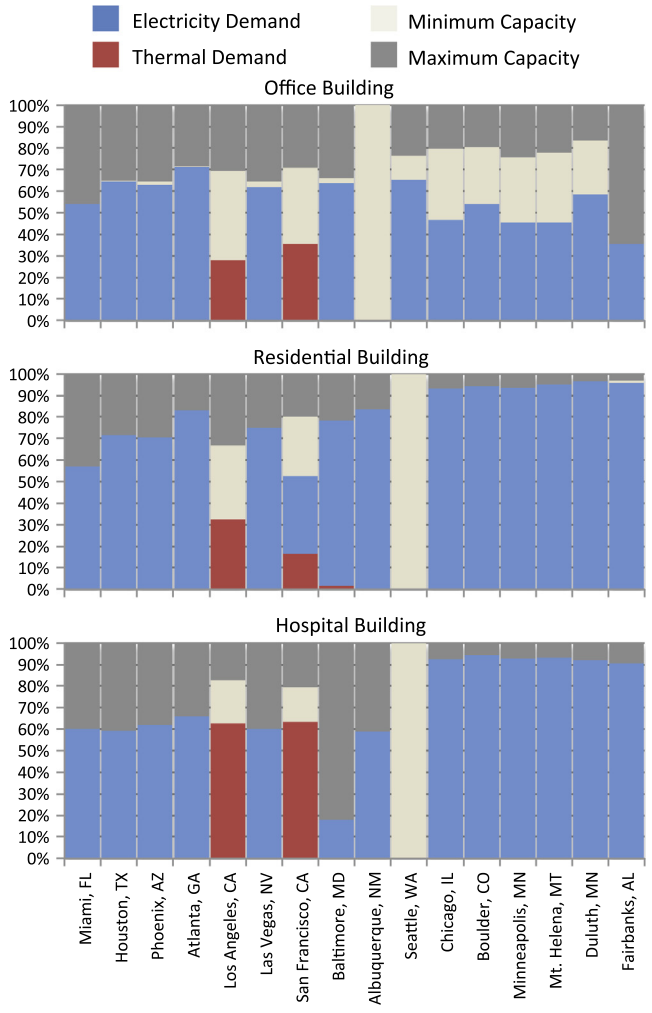

Fig. 13. Proportion of operating hours where CHP system is dispatched to meet the thermal demand, electrical demand, minimum CHP load, maximum CHP capacity for "Large" buildings under eGRID GHG emissions rates from grid electricity.

types in cold, very cold, and subarctic climates achieve reductions above 30% as these locations also have fairly high GHG emissions rates. The CHP Attributable reductions, however, range between 5 and 20%. The residential buildings in these locations consistently show above 15% CHP attributable reductions. With GHG emissions rates close to the break-even point, all buildings in located in Seattle, WA achieve very little GHG emissions reductions, less than 2%.

Lastly for the majority of building types, an electric load following heuristic best approximates the optimal operating strategy as shown in Fig. 13. The exceptions are for Los Angeles and San Francisco, CA where low GHG emissions rates and low thermal demands result in a thermal load following heuristic.

6. Conclusions

The goals of the current work were to ascertain the effects of building type, building size, climate and current GHG emissions from grid electricity on the GHG emission reductions possible from natural gas fueled building scale CHP systems. The reductions were estimated for prototypical hospitals, office, and residential buildings simulated in 16 different cities for microturbine, internal combustion engines, and phosphoric acid fuel cells. The results were also explored to understand the changes in system sizing and operation.

The analysis found that the fuel cell systems provided the largest GHG emissions reduction for the majority of building types in all climates under both "High" and "Low" GHG emissions rates from grid electricity. The exceptions where for "Large" Office and Hospital buildings in warm climates where the highest reductions were achieved with internal combustion engines with higher electrical efficiencies. Microturbines were the system of choice for "Large" and "Small" residential buildings in some cold, very cold and subarctic climates.

GHG emissions reductions for these prototypical buildings were between 30% and 47% under the "High" GHG emissions scenarios with residential buildings exhibiting the most variability with cities and the corresponding climates. Under the "Low" GHG emissions scenario, GHG emissions reductions for the majority of building types were less than 10%. Under "High" GHG emission scenarios the majority of GHG emissions reduction come from generating electricity more efficiently with a less carbon intensive fuel. This results in CHP Attributable reductions ranging between 1 and 20%, with residential buildings representing the higher end of the range.

In viewing the resulting CHP operation, the analysis found that the annual operating hours for Office and Residential buildings reduce under "Low" GHG emissions scenarios, as there must be a concurrent thermal and electrical demand to achieve GHG emissions reductions. Hospitals have concurrent thermal and electrical demands throughout the year therefore the operating hours do not diminish under lower GHG emissions scenarios.

In terms of operating strategy, under "High" GHG emissions scenarios, the optimal operating strategy is analogous to an electrical load following strategy, if operating. This is occurs due to the GHG emissions from grid electricity being higher than those produced from the CHP system. Under "Low" GHG emissions scenarios, the operating strategies vary, overall attempting to meet the *lower* of thermal and electric demands in any hour, if operating. This results in a thermal load following strategy for hospitals and office buildings in warm climates. For residential buildings in cold climates this leads to an electric load following strategy.

Considering current GHG emission rates for each location, the same trends were observed. A mixture of prime movers provided the largest GHG emissions reductions. Internal combustion engines were favored in locations with both high GHG emissions and electrical demands. Microturbines were the prime mover of choice for Seattle, WA where the GHG emissions coefficient is relatively low. Buildings in cold climates with high GHG emission rates where able to achieve GHG emissions reductions between 30 and 50%, however, the CHP attributable reductions where between 5 and 20%. The optimal operating strategy could be approximated with an electric load following heuristic for all locations and building types except for in locations with the lowest GHG emissions rates where a thermal load following approach is favored.

References

[1] Tan Wen-Shan, Hassan Mohammad Yusri, Shah Majid Md, Rahman Hasimah Abdul. Optimal distributed renewable generation planning: a review of different approaches. Renew Sustain Energy Rev 2013;18:626–45.

[2] Pepermans G, Driesen J, Haeseldonckx D, Belmans R, D'haeseleer W. Distributed generation: definition, benefits and issues. Energy Policy 2005;33(6):787–98.

[3] Chiradeja P, Ramakumar R. An approach to quantify the technical benefits of distributed generation. IEEE Trans Energy Convers 2004;19(4):764–73.

[4] Chicco Gianfranco, Mancarella Pierluigi. Distributed multi-generation: a comprehensive view. Renew Sustain Energy Rev 2009;13(3):535–51.

[5] Zhang Jian, Cho Heejin, Knizley Alta. Evaluation of financial incentives for combined heat and power (chp) systems in U.S. regions. Renew Sustain Energy Rev 2016;59:738–62.

[6] Kelly Scott, Pollitt Michael. An assessment of the present and future opportunities for combined heat and power with district heating (chp-dh) in the United Kingdom. Energy Policy 2010;38(11):6936–45. Energy efficiency policies and strategies with regular papers.

[7] Lemar Jr Paul L. The potential impact of policies to promote combined heat and power in {US} industry. Energy Policy 2001;29(14):1243–54. Scenarios for a clean energy future.

[8] Brown James E, Hendry Chris N, Harborne Paul. An emerging market in fuel cells? residential combined heat and power in four countries. Energy Policy 2007;35(4):2173–86.

[9] Brown Kevin, Minett Simon. History of chp developments and current trends. Appl Energy 1996;53(1–2):11–22. Combined heat and power in energy strategy and practice.

[10] Hinnells Mark. Combined heat and power in industry and buildings. Energy Policy 2008;36(12):4522–6. Foresight sustainable energy management and the built environment project.

[11] U.S. EPA. Catalog of CHP technologies. U.S. EPA; 2008. <http://www.epa.gov/chp/technologies.html>.

[12] Yun Kyungtae, Luck Rogelio, Mago Pedro, Smith Aaron. Analytic solutions for optimal power generation unit operation in combined heating and power systems. J Energy Resour Technol 2011;134.

[13] Hawkes AD, Leach MA. Cost-effective operating strategy for residential micro-combined heat and power. Energy 2007;32(5):711–23.

[14] Basrawi Firdaus, Ibrahim Thamir K, Habib Khairul, Yamada Takanobu. Effect of operation strategies on the economic and environmental performance of a micro gas turbine trigeneration system in a tropical region. Energy 2016;97:262–72.

[15] Mago Pedro J, Luck Rogelio, Smith Amanda D. Environmental evaluation of base-loaded chp systems for different climate conditions in the us. Int J Ambient Energy 2011;32(4):203–14.

[16] Knizley Alta, Mago Pedro J. Evaluation of combined heat and power (chp) systems performance with dual power generation units for different building configurations. Int J Energy Res 2013;37(12):1529–38.

[17] Mago Pedro J, Smith Amanda D. Evaluation of the potential emissions reductions from the use of chp systems in different commercial buildings. Build Environ 2012;53(0):74–82.

[18] Sundberg Gunnel, Henning Dag. Investments in combined heat and power plants: influence of fuel price on cost minimised operation. Energy Convers Manage 2002;43(5):639–50.

[19] Paepe Michel De, D'Herdt Peter, Mertens David. Micro-chp systems for residential applications. Energy Convers Manage 2006;47(18–19):3435–46.

[20] Pantaleo Antonio M, Camporeale Sergio, Shah Nilay. Natural gas–biomass dual fuelled microturbines: comparison of operating strategies in the italian residential sector. Appl Therm Eng 2014;71(2):686–96. Special issue: {MICROGEN} III: promoting the transition to high efficiency distributed energy systems.

[21] Ren Hongbo, Gao Weijun, Ruan Yingjun. Optimal sizing for residential chp system. Appl Therm Eng 2008;28(5–6):514–23.

[22] Ehyaei MA, Bahadori MN. Selection of micro turbines to meet electrical and thermal energy needs of residential buildings in Iran. Energy Build 2007;39(12):1227–34.

[23] Shaneb OA, Coates G, Taylor PC. Sizing of residential chp systems. Energy Build 2011;43(8):1991–2001.

[24] Ghadimi P, Kara S, Kornfeld B. The optimal selection of on-site {CHP} systems through integrated sizing and operational strategy. Appl Energy 2014;126(0):38–46.

[25] Howard Bianca, Saba Alexis, Gerrard Michael, Modi Vijay. Combined heat and power's potential to meet New York city's sustainability goals. Energy Policy 2014;65(0):444–54.
[26] Costa Antonio, Fichera Alberto. A mixed-integer linear programming (milp) model for the evaluation of chp system in the context of hospital structures. Appl Therm Eng 2014;71(2):921–9. Special issue: {MICROGEN} III: promoting the transition to high efficiency distributed energy systems.
[27] Cho Woojin, Lee Kwan-Soo. A simple sizing method for combined heat and power units. Energy 2014;65(0):123–33.
[28] Beihong Zhang, Weiding Long. An optimal sizing method for cogeneration plants. Energy Build 2006;38(3):189–95.
[29] Hueffed AK, Mago PJ. Influence of prime mover size and operational strategy on the performance of combined cooling, heating, and power systems under different cost structures. Proc Inst Mech Eng, Part A: J Power Energy 2010;224.
[30] Wang Jiang-Jiang, Jing You-Yin, Zhang Chun-Fa, Zhai Zhiqiang (John). Performance comparison of combined cooling heating and power system in different operation modes. Appl Energy 2011;88(12):4621–31.
[31] Pacific Northwest National Laboratory and Oak Ridge National Laboratory. Guide to determining climate regions by county. Technical report; August 2010.
[32] U.S. Department of Energy (US DOE). Commerical buildings initative: commerical reference building. U.S. Department of Energy (US DOE); 2011. <http://www1.eere.energy.gov/buildings/commercialinitiative/referencebuildings.html>.
[33] Energy Information Administration. Commercial building energy consumption survey. US Department of Energy; 2012.
[34] Ge jenbacher type 2 technical specifications. <http://site.ge-energy.com/prod_serv/products/recip_engines/en/downloads/ETS_E_T2_10_screen_August2010.pdf>.
[35] Ge jenbacher type 4 technical specifications. <http://site.ge-energy.com/prod_serv/products/recip_engines/en/type4.htm>.
[36] Ge jenbacher type 6 technical specifications. <https://www.ge-distributedpower.com/products/power-generation/up-to-5mw/jenbacher-type-6>.
[37] Catepillar gas generator set technical specifications. <http://www.cat.com/en_US/products/new/power-systems/electric-power-generation.html>.
[38] Capstone microturbine technical specifications. <http://www.capstoneturbine.com/_docs/Product%20Catalog_ENGLISH_LR.pdf>.
[39] Pure cell model 400 technical specifications. <http://www.doosanfuelcellamerica.com/energy/purecellmodel400system/>.
[40] Ren Hongbo, Gao Weijun. Economic and environmental evaluation of micro {CHP} systems with different operating modes for residential buildings in Japan. Energy Build 2010;42(6):853–61.